Journal of Inorganic and General Chemistry
ZAAC
Zeitschrift für anorganische und allgemeine Chemie
www.zaac.wiley-vch.de
RESEARCH ARTICLE

DOI: 10.1002/zaac.202200299

Room-Temperature Oxidation of Thulium-Metal Nanoparticles to the Thulium Oxocluster $[Tm_5O(O^iPr)_{13}]$

Andreas Reiß,[a] Sören Schlittenhardt,[b] Mario Ruben,[b, c, d] and Claus Feldmann*[a]

Dedicated to the late Professor Rudolf Hoppe on the occasion of his 100th birthday.

Zerovalent thulium nanoparticles (2.2 ± 0.3 nm in size) are used as the starting material to prepare single crystals of the thulium oxocluster $[Tm_5O(O^iPr)_{13}]$. The reaction is performed by controlled oxidation of the Tm(0) nanoparticles at room temperature (25°C) in isopropanol. The pentanuclear oxocluster contains a non-charged molecular unit with a central Tm_5O core and five μ_1-, four μ_2-, and four μ_3-bridging $(O^iPr)^-$ ligands. Single-crystal structure analysis ($P2_1/n$, $a = 1247.7(6)$, $b = 2146.2(15)$, $c = 2056.6(9)$ pm, $\beta = 93.23(1)°$) and infrared spectroscopy confirm the oxidation of HO^iPr with formation of H_2 and $(O^iPr)^-$. Temperature-dependent measurements show antiferromagnetic coupling. Such a polynuclear $[Ln_5O(O^iPr)_{13}]$ oxocluster (*Ln:* lanthanide) is prepared with thulium-metal nanoparticles as a starting material for the first time and points to the suitability of reactive rare-earth metal nanoparticles as starting materials.

1. Introduction

In contrast to thulium bulk metal, thulium-metal nanoparticles could be reacted in the liquid phase with quasi homogeneous conditions. Bulk thulium is usually less reactive due to its low surface area as well as due to surface passivation layers (e.g., thulium oxide, thulium hydroxide, thulium carbonate).[1] Purification of bulk thulium is elaborate and requires high-temperature sublimation.[1,2] Knowledge on zerovalent thulium (Tm(0)) nanoparticles, however, is rare and limited to ball milling until now.[3] In the literature, thulium-containing nanoparticles usually relate to metal oxides or metal halides that are doped with Tm^{3+} in order to establish Tm^{3+}-based luminescence, specifically including up-conversion processes.[4] A liquid-phase synthesis of Tm(0) nanoparticles, to the best of our knowledge, was not reported until now, which can be ascribed to the high reactivity in relation to the position of thulium in the voltage series with a standard potential (E_0) of −2.3 V of the bulk metal.[5] Due to the small size and the great number of surface atoms, in fact, the reactivity of nanosized Tm can be expected even to be significantly higher as compared to the bulk metal. To this concern, we could recently realize nanoparticles of all rare-earth metals for the first time by reduction of metal halides with lithium or sodium naphthalenide ([LiNaph], [NaNaph]) in the liquid phase (THF).[6]

Pentanuclear oxoclusters $[Ln_5O(O^iPr)_{13}]$ (*Ln*: lanthanide) are already known, preferentially for the lighter lanthanide metals (i.e., La–Nd, Eu, Gd, Dy, Ho, Er, Yb), and were predominately realized by Westin *et al.*[7] Their magnetic properties can be very interesting and specifically $[Ho_5O(O^iPr)_{13}]$ and $[Dy_5O(O^iPr)_{13}]$ discovered by Winpenny *et al.* represent single-molecule magnets with high energy barriers of 400 K (Ho) and 530 K (Dy).[8] Beside their crystal structure[7] and luminescence properties,[7b–d] however, the magnetic properties of several $[Ln_5O(O^iPr)_{13}]$ oxoclusters were not examined until now (i.e., Ce, Pr, Nd, Eu, Tm, Yb, Lu). Beside their magnetic features, rare-earth-metal alkoxides can also be relevant for obtaining rare-earth-metal oxide thinfilms or nanoparticles.[9] The synthesis of the oxoclusters was yet typically performed by reacting KO^iPr and $LnCl_3$ in toluene,[7a] which often also results in other insoluble lanthanide oxide alkoxides as side products. By controlled oxidation of Tm(0) nanoparticles in isopropanol (HO^iPr), we can now prepare $[Tm_5O(O^iPr)_{13}]$ at room temperature. Such formation of a multinuclear oxocluster by direct reaction of rare-earth metal nanoparticles and the alcohol is shown for the first time. The title compound is characterized by single-crystal structure

[a] *A. Reiß, Prof. Dr. C. Feldmann*
Institut für Anorganische Chemie,
Karlsruhe Institute of Technology (KIT),
Engesserstraße 15, D-76131
Karlsruhe (Germany)
E-mail: claus.feldmann@kit.edu
[b] *S. Schlittenhardt, Prof. Dr. M. Ruben*
Institute of Nanotechnology,
Karlsruhe Institute of Technology (KIT),
76021 Karlsruhe (Germany)
[c] *Prof. Dr. M. Ruben*
Institute for Quantum Materials and Technologies (IQMT),
Karlsruhe Institute of Technology (KIT),
Karlsruhe (Germany)
[d] *Prof. Dr. M. Ruben*
Centre Européen de Sciences Quantiques (CESQ),
Institut de Science et d'Ingénierie,
Supramoléculaire (ISIS), Université de Strasbourg,
Strasbourg (France)

Supporting information for this article is available on the WWW under https://doi.org/10.1002/zaac.202200299

analysis, elemental analysis, infrared spectroscopy, and magnetic measurements.

2. Results and Discussion

2.1. Thulium-metal nanoparticles

The synthesis of the Tm(0) nanoparticles is performed using $TmCl_3$ as starting material and lithium naphthalenide, [LiNaph], as reducing agent as well as tetrahydrofuran as the solvent (Figure 1). Due to the low solubility of $TmCl_3$ in THF, a one-pot approach is applied with $TmCl_3$, lithium metal and naphthalene added to THF (Figure 1a). Whereas naphthalene is soluble in THF, $TmCl_3$ largely remains as an insoluble solid at the bottom of the glass tube. Lithium metal is located on top of the liquid phase due to its low density. Upon intense stirring for 12 hours, first of all, [LiNaph] is formed resulting in a greenish solution. Moreover, $TmCl_3$ is slowly dissolved and instantaneously reacts with [LiNaph] to form Tm(0) nanoparticles. Although the nanoparticle nucleation is performed with, from a general perspective, the disadvantageous conditions of an inhomogeneous system (i.e., lithium and $TmCl_3$ as solids), two essential aspects nevertheless promote the nucleation of very small nanoparticles. First of all, the reduction of $TmCl_3$ by [LiNaph] is very fast. Furthermore, the solubility of thulium metal in THF is extremely low, so that a sufficient supersaturation is achieved.[6,10] After 12 hours of vigorous stirring, $TmCl_3$ and lithium metal have reacted completely, resulting in a deep black suspension of Tm(0) nanoparticles (Figure 1b).

The Tm(0) nanoparticles were purified by centrifugation and repeated redispersion/centrifugation in/from a mixture of THF and toluene (1 : 1). Thereafter, they can be either redispersed in THF or dried in vacuum to obtain colloidally stable suspensions or powder samples. Caution needs to be paid for the handling of the Tm(0) nanoparticles. Thus, Tm(0) nanoparticle suspensions and powder samples are highly reactive when in contact with O_2, H_2O or other oxidizing agents.[6] Specifically, the reaction of powder samples with oxygen and/or water can result in a sting flame and explosion. Therefore, the nanoparticles need to be handled and stored under inert conditions (argon, nitrogen).

Particle size and particle shape of the Tm(0) nanoparticles were examined by transmission electron microscopy (TEM). Accordingly, spherical nanoparticles with uniform size were obtained with a size range of 1–3 nm and a low degree of agglomeration (Figure 2a). Statistical evaluation of >250 nanoparticles on TEM images resulted in a mean diameter of 2.2 ± 0.3 nm (Figure 2c). High-resolution (HR)TEM images prove the as-prepared Tm(0) nanoparticles to be monocrystalline with

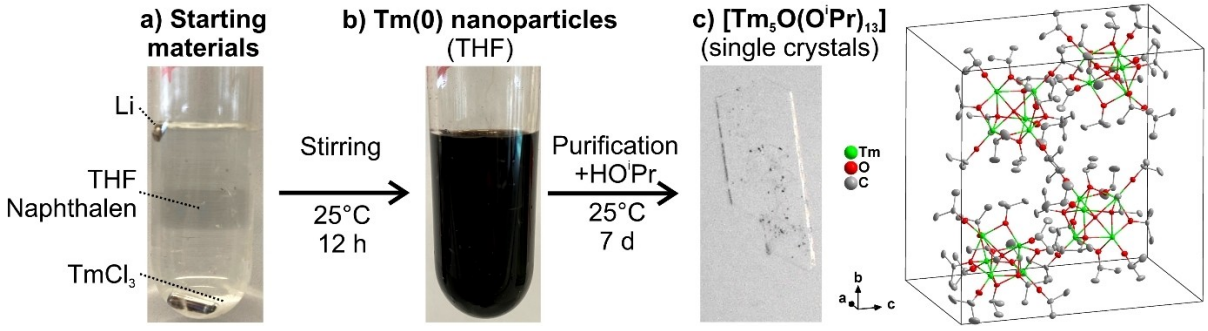

Figure 1. Scheme illustrating the synthesis of Tm(0) nanoparticles with a) starting materials, b) the as-prepared Tm(0) nanoparticles in THF, c) single crystal and unit cell of $[Tm_5O(O^iPr)_{13}]$ after oxidation of Tm(0) nanoparticles with isopropanol (HO^iPr).

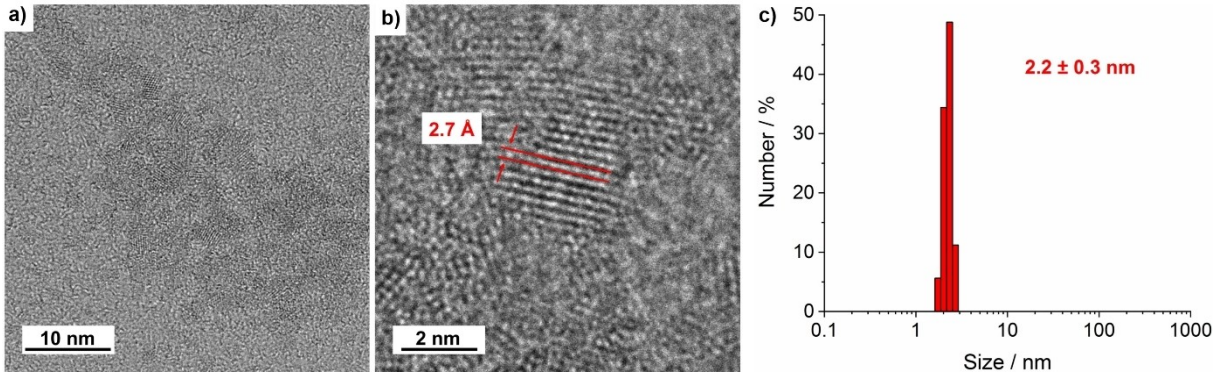

Figure 2. Electron microscopy of the as-prepared Tm(0) nanoparticles: a) TEM overview image, b) single Tm(0) nanoparticle with lattice fringes, c) size distribution (based on statistical evaluation of >250 nanoparticles on TEM images).

lattice fringes through the whole particle (Figures 2b). The lattice plane distance of 2.7 ± 0.1 Å is in good agreement with hexagonal bulk thulium (Tm(0): $d_{11\text{-}1}$ with 2.693 Å).[11]

Composition and surface functionalization of the as-prepared Tm(0) nanoparticles were examined by X-ray powder diffraction (XRD) and Fourier-transform infrared (FT-IR) spectroscopy after purification via repeated centrifugation/redispersion in/from a THF/toluene mixture (1 : 1) and drying in vacuum to obtain powder samples (Figure 3). XRD only shows two broad Bragg reflexes with low intensity at two-theta angles of 30 and 60° (Figure 3a). In regard of a slow reaction (12 hours) at low temperature (25 °C), it is a surprise to observe Bragg reflexes and certain crystallinity at all. The observed Bragg reflexes, in fact, fit well with a reference diffractogram of bulk thulium metal. According the Scherrer formalism, a mean crystallite size of 2.4 nm was deduced for the Tm(0) nanoparticles, which is well in agreement with the particle diameter obtained from electron microscopy. In sum, XRD and HRTEM confirm the presence of monocrystalline Tm(0) nanoparticles. FT-IR spectra indicate the molecules adsorbed on the particle surface. Accordingly, THF and toluene as the solvents and naphthalene as remain of the reducing agent can be expected. Upon comparing with reference spectra, it turned out that the Tm(0) nanoparticles only show weak absorptions related to THF (ν(C–H): 3000–2800 cm^{-1}, ν(C–O): 1050–800 cm^{-1}) and naphthalene (1600–800 cm^{-1}) (Figure 3b).

2.2. Reaction with isopropanol

Thulium-metal nanoparticles are generally highly reactive when in contact to oxidizing agents. Especially, powder samples show spontaneous ignition and explosion when in contact to oxygen or water. On the other hand, Tm(0) suspensions in THF are colloidally and chemically highly stable when stored under inert conditions (N_2, Ar). To probe the reactivity of rare-earth metal nanoparticles in general, we have already reacted them in the liquid phase near room temperature (≤ 100 °C) with conventional strongly oxidizing agents such as O_2, H_2O, S_8, or I_2. As a result, nanosized as well as single crystalline compounds were obtained at temperatures of 20 to 80 °C.[6] For the exploration of the reactivity and the reactions of the novel rare-earth metal nanoparticles, several questions are most relevant: *i*) Is the oxidation controllable in the liquid phase near room temperature in view of a formation and crystallization of specific compounds? Do the starting materials and solvents applied for the synthesis of the metal nanoparticles influence or even deteriorate the reactions and product formation? Are new compounds with interesting binding, structure, and/or properties obtainable?

In view of the aforementioned questions, we have here exemplarily reacted Tm(0) nanoparticles with isopropanol. Due to the high reactivity of the nanoparticles, the reaction of dried Tm(0) nanoparticles occurs after addition of few drops of HO^iPr at room temperature and results in the formation of colorless single crystals with good yield (60 %) (Figure 1c). According to X-ray structure analysis, the single crystals exhibit the monoclinic space group $P2_1/n$, and the obtained compound has a composition $[Tm_5O(O^iPr)_{13}]$ (Table 1).

The title compound consists of non-charged, molecular $[Tm_5O(O^iPr)_{13}]$ units arranged in a face-centered cubic packing in the solid state (Figure 1c). The cage-like molecular units consist of five Tm atoms, each of them coordinated by one μ_1- and four μ_2- or μ_3-coordinating $(O^iPr)^-$ ligands (Figure 4a). Finally, all Tm atoms are coordinated by a central oxygen atom. Thus, all thulium atoms are in the trivalent oxidation state, and they have a strongly distorted octahedral coordination. Besides the μ_1-$(O^iPr)^-$ ligands at each Tm atom, four μ_3-coordinating $(O^iPr)^-$ ligands are located at the top of the cage-like oxocluster and four μ_2-$(O^iPr)^-$ ligands are positioned at the bottom of the molecule (Figure 4b). The Tm–O distances range from 201.2(5)–204.0(5) pm for μ_1-(O^iPr), 218.7(5)–221.9(5) pm for μ_2-(O^iPr),

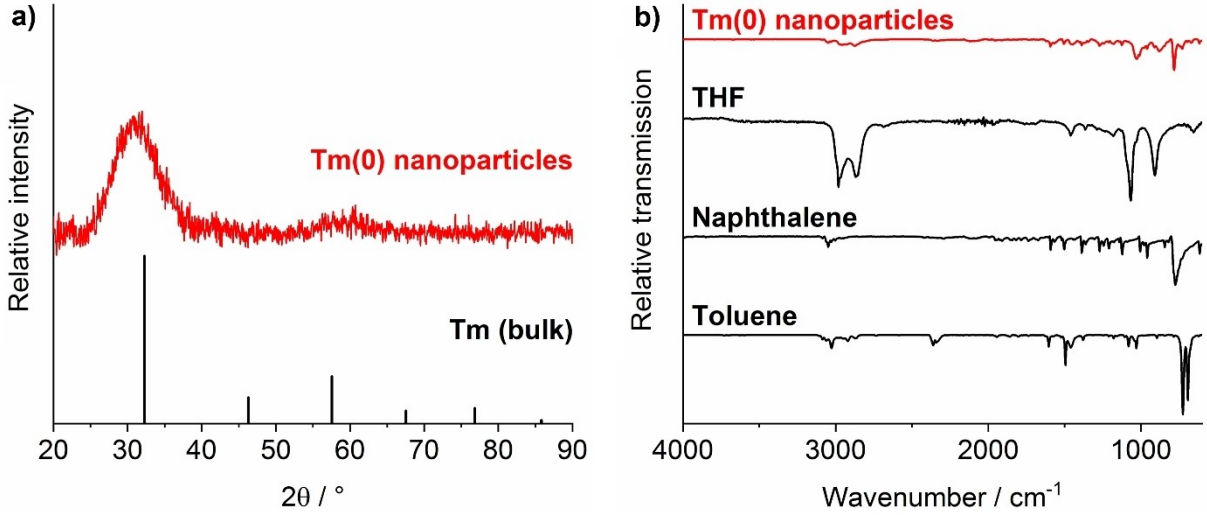

Figure 3. Composition and surface functionalization of the as-prepared Tm(0) nanoparticles: a) XRD (bulk thulium as a reference: ICDD-No. 03-065-4993), b) FT-IR spectrum with THF, toluene, and naphthalene as references.

Table 1. Crystallographic data and refinement details of $[Tm_5O(O^iPr)_{13}]$.

Data	$Tm_5O(O^iPr)_{13}$
Sum formula	$C_{39}H_{91}O_{14}Tm_5$
Crystal system	Monoclinic
Space group	$P2_1/n$
Lattice parameters	$a = 1247.7(6)$ pm $b = 2146.2(15)$ pm $c = 2056.6(9)$ pm $\beta = 93.28(4)°$
Cell volume	$V = 5498(5) \times 10^6$ pm^3
Formula units per cell	$Z = 4$
Calculated density	$\rho = 1.968$ g cm^{-3}
Measurement limits	$-15 \le h \le 15$, $-26 \le k \le 26$, $-25 \le l \le 25$
Theta range for data collection	1.89 to 26.02°
Linear absorption coefficient	$\mu = 8.036$ mm^{-1}
Number of reflections	61466 (10842 independent)
Refinement method	Full-matrix least-squares on F^2
Merging	$R_{int} = 0.070$
Number of parameters	549
Residual electron density	1.62 to -1.50 e$^- \cdot 10^{-6}$ pm^{-3}
R_1 ($I \ge 2\sigma_I$)	0.042
R_1 (all data)	0.067
wR_2 (all data)	0.103
GooF	0.938

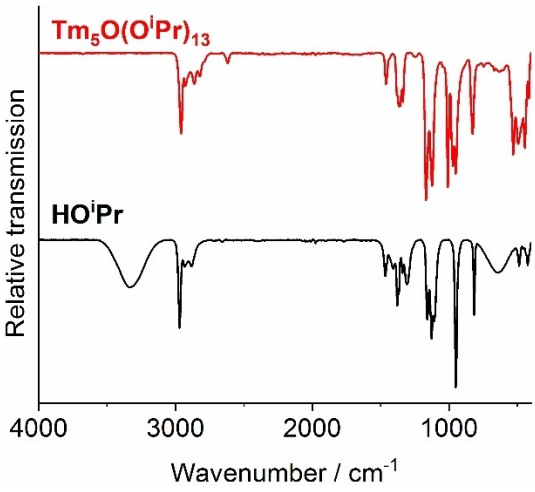

Figure 5. FT-IR spectrum of $[Tm_5O(O^iPr)_{13}]$ with isopropanol as a reference.

226.8(5)–240.8(5) pm for μ_3-(O^iPr), and 229.9(5)–233.5(5) for the μ_4-coordinating oxygen atom (Figure 4b). The increase of the Tm–O distances, as expected, reflects the increasing coordination of the ligands. Moreover, these distances are similar to those in the known $[Ln_5O(O^iPr)_{13}]$ oxoclusters (i.e., La–Nd, Eu, Gd, Dy, Ho, Er, Yb).[7,8]

Composition and bonding of $[Tm_5O(O^iPr)_{13}]$ were further examined by Fourier-transformed infrared (FT-IR) spectroscopy and elemental analysis (EA). FT-IR spectra of $[Tm_5O(O^iPr)_{13}]$ show the expected vibrations of the $(O^iPr)^-$-ligands, which are well in agreement with the HO^iPr reference spectrum (Figure 5). Due to the different lattice symmetry of the $(O^iPr)^-$ ligands in the solid state, spectra of the title compound show a more pronounced splitting of vibrations as compared to the reference. Most important, the absence of any O–H vibration (3600–3000 cm^{-1}) in the spectrum of $[Tm_5O(O^iPr)_{13}]$ points to the absence of OH^- and/or H_2O and a complete deprotonation of all $(O^iPr)^-$ ligands. According to EA (C/H analysis), the experimental findings (29.1% C, 5.4% H, remain of Tm/O: 65.5%) are well in agreement with the calculated values (28.8% C, 5.6% H, remain of Tm/O: 65.6%), which confirms the composition of the title compound. Finally, an X-ray diffractogram of a powder sample is in good agreement with a diffractogram calculated from the data of the single-crystal structure analysis. Due to the pronounced heavy-atom structure with a few high-intensity reflexes at two-theta $< 10°$ and a great number of overlapping weak reflexes at two-theta $> 10°$ (*SI: Figure S1*), however, the significance of the powder data is limited. Together with single-crystal structure analysis, FT-IR and EA confirm the composition of the title compound with Tm^{3+} cations as well as with $(O^iPr)^-$ ligands and

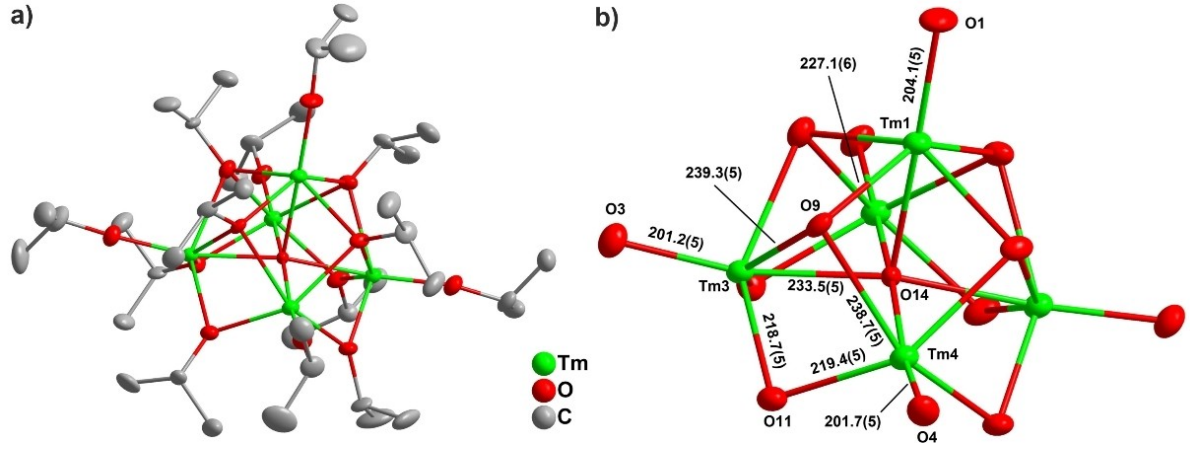

Figure 4. Molecular structure of $[Tm_5O(O^iPr)_{13}]$ (a) and central oxocluster with distances in pm (b).

a central oxide atom. All-in-all, the formation of the title compound can be ascribed to the following reaction:

$$5\ Tm + 15\ HO^iPr \rightarrow [Tm_5O(O^iPr)_{13}] + O(^iPr)_2 + 15/2\ H_2$$

The composition $[Tm_5O(O^iPr)_{13}]$ with the cage-like Tm_5O core is obviously specifically stable, and although predominately known for the lighter rare-earth metals here first obtained for thulium. The occurrence of a single oxygen atom can be ascribed to the Lewis acidity of the Tm^{3+} cations and their high charge, which require the presence of a high-charged O^{2-}. In regard of the reactivity and reactions of the Tm(0) nanoparticles, it is most important to notice that a multinuclear oxocluster can be formed and crystallized at room temperature without any ingredients of the initial Tm(0)-nanoparticle synthesis, such as THF, toluene, naphthalene, or LiCl.

In regard of a pentanuclear oxocluster with a great number of *f*-electrons and the potentially promising magnetic properties, and specifically, the single-molecule magnets $[Ho_5O(O^iPr)_{13}]$ and $[Dy_5O(O^iPr)_{13}]$,[8] we have examined the magnetism of $[Tm_5O(O^iPr)_{13}]$. Temperature-dependent measurements of the susceptibility over the temperature range 2–300 K were carried out (Figure 6). At room temperature, a χT value of 24 cm^3 K mol^{-1} was measured, which is lower than expected for five independent Tm^{3+} cations (35.7 cm^3 K mol^{-1}). This finding can be ascribed to remaining solvent adhered on the crystal surfaces. On cooling, χT decreases slowly at first, and then faster below 25 K, reaching 6 cm^3 K mol^{-1} at 2 K. This probably indicates a combination of thermal depopulation of the m_J sublevels and antiferromagnetic coupling between the Tm^{3+} centers. To check for possible SMM behavior, *a.c.* susceptibility measurements were carried out, but no "out-of-phase χ" signals were observed.

3. Conclusion

Although polynuclear lanthanide (*Ln*) oxoclusters with a composition $[Ln_5O(O^iPr)_{13}]$ and a central Ln_5O unit are known predominately for the lighter lanthanides, the thulium oxocluster $[Tm_5O(O^iPr)_{13}]$ has not been realized until now. Generally, such oxocluster was prepared using Tm(0) nanoparticles as the starting material, for the first time. These Tm(0) nanoparticles (2.2 ± 0.3 nm in size) were prepared by a one-pot reduction of $TmCl_3$ with [LiNaph] in THF. Thereafter, the Tm(0) nanoparticles were centrifuged, washed by redispersion/centrifugation in/from a THF/toluene mixture, dried in vacuum at room temperature and thereafter reacted with isopropanol. Single crystals of $[Tm_5O(O^iPr)_{13}]$ were obtained with good yield (60 %) at room temperature. The title compound contains a square-pyramidal pentanuclear oxocluster with a central Tm_5O core as well as five μ_1-, four μ_2-, and four μ_3-$(O^iPr)^-$ ligands coordinating Tm^{3+}. Beside single-crystal structure analysis, infrared spectroscopy evidences the deprotonation of HO^iPr. Temperature-dependent measurements show antiferromagnetic coupling. In sum, synthesis and compound show the feasibility of Tm(0) nanoparticles for reactions at the border of homogeneous and heterogeneous conditions and the crystallization of complex compounds near room temperature (≤ 100 °C).

Experimental

Material synthesis

Chemicals. Tetrahydrofuran (THF, Seulberger, 99%) and toluene (Seulberger, 99%) were refluxed under argon atmosphere over sodium with benzophenone as indicator and distilled off prior to use. Isopropanol (Seulberger, 99%) was degassed under nitrogen

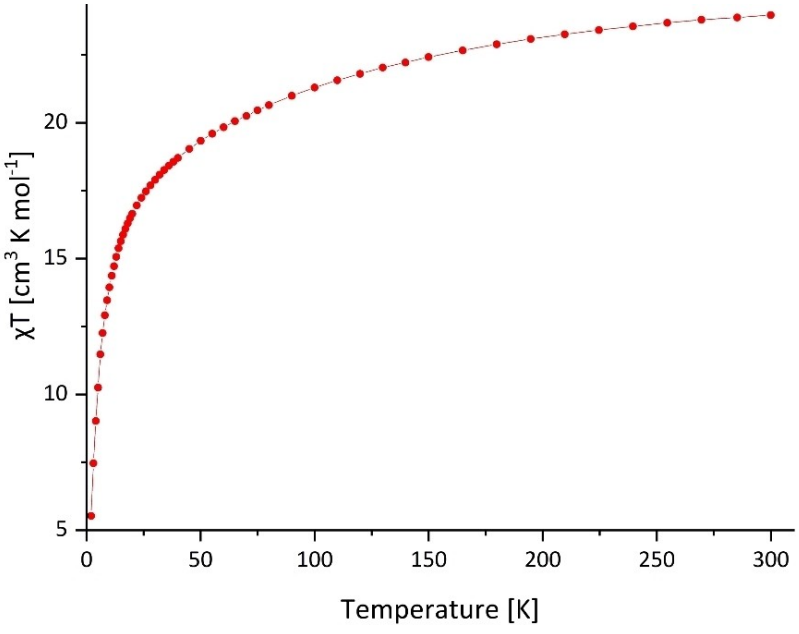

Figure 6. Magnetic properties of $[Tm_5O(O^iPr)_{13}]$.

atmosphere and dried for one month over molecular sieve. Lithium metal (Alfa Aesar, 99%) was freshly cut under argon atmosphere prior to use. Naphthalene (Alfa Aesar, $\geq$99%) and $TmCl_3$ (Sigma-Aldrich, 99.9%) were used as purchased.

Tm(0) nanoparticles. 6.9 mg of lithium (1.00 mmol), 134.6 mg of naphthalene (1.05 mmol) and 90.8 mg of $TmCl_3$ (0.33 mmol) were reacted in 15 mL THF and stirred for 12 hours at 25 °C to form Tm(0) nanoparticles in a one-pot approach. The formation of Tm(0) nanoparticles was indicated by the change from colorless to a deep black suspension. Thereafter, 10 mL of toluene were added to the obtained Tm(0) nanoparticle suspension before separating the nanoparticles by centrifugation (42,500×g) and purified by washing with 15 mL of a 1:1 mixture of toluene and THF. Finally, the Tm(0) nanoparticles were redispersed in THF to obtain long-term stable suspensions or dried in vacuum to obtain powder samples with a yield of about 60%.

$[Tm_5O(O^iPr)_{13}]$. 31.2 mg of washed and dried Tm(0) nanoparticles (0.185 mmol Tm) and 0.3 mL of isopropanol were added into a glass ampoule. This glass ampoule was sealed under inert conditions and stored for seven days at room temperature. After this time, colorless, thin crystals of $[Tm_5O(O^iPr)_{13}]$ were obtained. The reaction is assumed to proceed quantitatively as no black Tm(0) nanoparticles remain thereafter.

Analytical techniques

Transmission electron microscopy. For TEM sample preparation, diluted suspensions of the as-prepared Tm(0) nanoparticles in THF were deposited and evaporated on a commercial 400 µm mesh Cu-grid (Plano 01824) covered by a holey amorphous carbon film with a nominal thickness of 3 nm. To avoid any oxidation during TEM sample preparation, the nanoparticle deposition on the carbon (lacey-)film copper grids was performed under argon atmosphere in a glovebox. Thereafter, the grids were transferred with a suitable vacuum/inert gas transfer module (GATAN transfer module) into the transmission electron microscope without any contact to air. TEM and high-resolution (HR)TEM were conducted with a FEI Osiris microscope operated at 200 kV and a FEI Titan^3 80-30 operated at 300 keV.

X-ray powder diffraction (XRD) was performed on a STOE STADI-MP diffractometer operating with Ge-monochromatized Cu–K_α-radiation (λ = 1.54178 Å). Powder samples of the Tm(0) nanoparticles were diluted with dried glass spheres (9–13 µm, Sigma-Aldrich) to reduce the X-ray absorption of the nanoparticles and filled into glass capillaries under argon. Since the scattering power of the metal nanoparticles (diameter $\leq$10 nm) is low, certain non-specific background occurs, which was fitted by background correction (Win-XPOW, 1.2v).

Fourier-transform infrared (FT-IR) spectra were recorded on a Bruker Vertex 70 FT-IR spectrometer (Bruker). The samples were measured as pellets in KBr. Thus, 300 mg of dried KBr and 0.5–1.0 mg of the title compound were carefully pestled together and pressed to a thin pellet.

Elemental analysis (EA) (C/H analysis) of $[Tm_5O(O^iPr)_{13}]$ was performed via thermal combustion with an Elementar Vario Microcube device (Elementar, Germany) at a temperature of about 1100 °C.

Crystal structure determination and refinement. For single crystal structure analysis, suitable crystals of $[Tm_5O(O^iPr)_{13}]$ were selected manually, covered by inert-oil (perfluoropolyalkylether, ABCR), and deposited on a micro gripper (MiTeGen). Data collection of $Tm_5O(O^iPr)_{13}$ was performed at 100 K with a Stoe StadiVari Diffractometer with Euler geometry (Stoe, Darmstadt) using Mo–K_α radiation (λ = 0.71073 Å, graphite monochromator).

Data reduction and multi-scan absorption correction were conducted by the X-AREA software package and Stoe LANA (version 1.75).[12] Space group determination based on systematic absence of reflections was performed by XPREP. Using Olex2,[13] the structures were solved with the ShelXS[14] structure solution program with Direct Methods and refined with the ShelXL[14] refinement package using least squares minimization. All non-hydrogen atoms were refined anisotropically. Details of structure determination and structure refinement are listed in Table 1. DIAMOND was used for all illustrations.[15] Refinement was checked with PLATON.[16] Further details related to the crystal structures may be obtained from the joint CCDC/FIZ Karlsruhe deposition service on quoting the depository number 2204615.

Magnetism. Magnetic measurements were performed with a Quantum Design MPMS-XL SQUID magnetometer on a ground polycrystalline sample immobilized in eicosane. Corrections for sample holder and diamagnetic contribution were applied.

Supporting Information

Data related to X-ray powder diffraction of $[Tm_5O(O^iPr)_{13}]$ are deposited in the Supporting Information.

Acknowledgements

The authors are grateful to the Deutsche Forschungsgemeinschaft (DFG) for funding of personnel (NanoMet: FE911/11-1, GE 841/29-1) and TEM equipment (INST 121384/33-1 FUGG). Furthermore, the authors thank Prof. Dr. Peter Roesky and Dr. Michael Gamer for data collection on a Stoe Stadi Vari diffractometer. Open Access funding enabled and organized by Projekt DEAL.

Conflict of Interest

The authors declare no conflict of interest.

Data Availability Statement

The data that support the findings of this study are available from the corresponding author upon reasonable request.

Keywords: Thulium nanoparticles · multinuclear oxocluster · isopropanol · crystal structure · liquid-phase

[1] D. A. Atwood, in *The Rare Earth Elements: Fundamentals and Applications*, Wiley-VCH, Weinheim **2012**.
[2] G. Brauer, *Handbuch der präparativen Anorganischen Chemie*, Enke, Stuttgart **1978**, Vol. 2, pp. 1071.
[3] Y. Saito, *Carbon* **1995**, *33*, 979–988.

[4] G. Tessitore, S. L. Maurizio, T. Sabri, J. A. Capobianco, *Angew. Chem. Int. Ed.* **2019**, *58*, 9742–9751; *Angew. Chem.* **2019**, *131*, 9844–9853.
[5] N. Wiberg, E. Wiberg, A. F. Holleman, in *Anorganische Chemie*, de Gruyter, Berlin **2017**, 103. Ed., Vol. 1, Annex III/IV.
[6] D. Bartenbach, O. Wenzel, R. Popescu, L.-P. Faden, A. Reiß, M. Kaiser, A. Zimina, J.-D. Grunwaldt, D. Gerthsen, C. Feldmann, *Angew. Chem. Int. Ed.* **2021**, *60*, 17373–17377.
[7] a) M. Kritikos, M. Moustiakimov, G. Westin, *Inorg. Chim. Acta* **2012**, *384*, 125–132; b) G. Westin, M. Moustiakimov, M. Kritikos, *Inorg. Chem.* **2002**, *41*, 3249–3258; c) M. Kritikos, M. Moustiakimov, M. Wijk, G. Westin, *J. Chem. Soc. Dalton Trans.* **2001**, 1931–1938; d) G. Westin, M. Kritikos, M. Wijk, *J. Solid State Chem.* **1998**, *141*, 168–176; e) L. G. Hubert-Pfalzgraf, S. Daniele, A. Bennaceur, J.-C. Daranbt, J. Vaissermann, *Polyhedron* **1997**, *16*, 1223–1234; f) D. C. Bradley, H. Chudzynska, D. M. Frigo, M. E. Hammond, M. B. Hursthouse, M. A. Mazid, *Polyhedron* **1990**, *9*, 719–726.
[8] a) R. J. Blagg, F. Tuna, E. J. L. McInnes, R. E. P. Winpenny, *Chem. Commun.* **2011**, *47*, 10587–10589; b) R. J. Blagg, C. A. Muryn, E. J. L. McInnes, F. Tuna, R. E. P. Winpenny, *Angew. Chem. Int. Ed.* **2011**, *50*, 6530–6533; *Angew. Chem.* **2011**, *123*, 6660–6663.
[9] a) M. Veith, S. Mathur, H. Shen, N. Lecerf, S. Huefner, M. H. Jilavi, *Chem. Mater.* **2001**, *13*, 4041–4052; b) M. Veith, *J. Chem. Soc. Dalton Trans.* **2002**, *12*, 2405–2412.
[10] V. K. LaMer, R. H. J. Dinegar, *J. Am. Chem. Soc.* **1950**, *72*, 4847–4854.
[11] F. H. Spedding, A. H. Daane, K. W. Herrmann, *Acta Crystallogr.* **1956**, *9*, 559–563.
[12] J. Koziskova, F. Hahn, J. Richter, J. Kožíšek, *Acta Chim. Slov.* **2016**, *9*, 136–140.
[13] V. Dolomanov, L. J. Bourhis, R. J. Gildea, J. A. K. Howard, H. Puschmann, *J. Appl. Crystallogr.* **2009**, *42*, 339–341.
[14] a) G. M. Sheldrick, *Acta Crystallogr.* **2015**, *C71*, 3–8; b) G. M. Sheldrick, *Acta Crystallogr.* **2008**, *A64*, 112–122.
[15] DIAMOND Version 4.2.2 – *Crystal and Molecular Structure Visualization*, Crystal Impact GbR, Bonn, 2016.
[16] a) A. L. Spek, *Acta Crystallogr.* **2015**, *C71*, 9–18; b) A. L. Spek, *Acta Crystallogr.* **2009**, *D65*, 148–155.

Manuscript received: September 12, 2022
Revised manuscript received: November 16, 2022
Accepted manuscript online: November 18, 2022

